

# High $p_T$ Probes of Dense Matter Created in Heavy Ion Collisions at RHIC

B.A. Cole <sup>a</sup>

<sup>a</sup> Dept. of Physics, Columbia University and Nevis Laboratories  
P.O. Box 137, Irvington, NY 10533

An overview of recent high- $p_T$  hadron and photon measurements at RHIC is presented with a focus on the evolution of hadron/photon production from intermediate  $p_T$  ( $\lesssim 5$  GeV/c) to high  $p_T$  ( $> 10$  GeV/c). Addressed topics include single high- $p_T$  hadron production, azimuthal anisotropy of  $\pi^0$  production, di-jet modification at intermediate  $p_T$  and inclusive photon-hadron correlations. The understanding of these results in the context of different energy loss models is also discussed.

## 1. Introduction

The study of high- $p_T$  particle production is one of the most important components of the ultra-relativistic heavy ion program at RHIC. The phenomenon of jet quenching in Au+Au collisions at RHIC is now clearly established by measurements of single hadron suppression and di-jet quenching together with control measurements in d+Au collisions (see [1–4] and references therein). Recent results [5] showing that the prompt photon yields in Au+Au collisions are consistent with pQCD expectations have provided ultimate proof that hard scattering processes occur at the expected rate in Au+Au collisions and that the observed jet quenching is a final-state effect. The above described results have been used to obtain estimates of primordial parton number and energy densities [6–8] that are well in excess of the densities required for quark-gluon plasma formation. Jet quenching is one of the key observations supporting the conclusion that Au+Au collisions at RHIC produce a strongly coupled quark-gluon plasma [9–13,7,14,15]. More recent measurements indicating possible longitudinal flow effects on parton propagation and fragmentation [16] and observations of a strongly modified di-jet shape at intermediate  $p_T$  [17] suggest that high- $p_T$  measurements at RHIC may soon provide sensitivity to medium properties beyond color-charge density.

In spite of the above-described successes, there are a number of open issues with our understanding of the energy loss process. While most energy loss calculations consider only radiative energy loss [18–22], recent analyses suggest that collisional energy loss could contribute significantly in the currently accessible momentum range [23,24] – particularly for heavy quarks [25,26]. Also, very recent analyses of the parton cascade in the medium [27] may provide a completely new view of “jet quenching” physics. Given the sQGP interpretation, we may also have to consider radically different quenching mechanisms [28]. There is even some uncertainty about the dominance of hard scattering contributions to hadron production at transverse momenta normally considered to be high [29,30].

Furthermore, measurements of the azimuthal anisotropy of high- $p_T$  hadron production demonstrate that physics beyond “ordinary” radiative energy loss must contribute over a large part of the currently accessible  $p_T$  range, since radiative energy loss calculations cannot yet explain [31–34] the large observed hadron  $v_2$  values without invoking “extra” physics such as recombination [33,35,36], larger energy loss for partons crossing the flow field [37], or other new mechanisms (e.g. [28,30,38]). Thus, we cannot be certain that the radiative energy loss is truly the dominant physics process driving the observed hadron suppression over the accessible  $p_T$  range.

Another potentially serious problem with our understanding of jet quenching arises from differences of interpretation of the single hadron data. In particular, analyses using BDMPS quenching weights [39,40] have suggested that the medium in Au+Au collisions is sufficiently opaque that the single hadron suppression measurements are only sensitive to jets produced at the very edge of the collision zone and that unexpectedly large in-medium scattering cross-sections may be required to describe the data. While it has been argued that effects of transverse expansion on the medium-induced energy loss can account for the apparent opacity [41], other calculations [6,42,43] are capable of describing single-hadron measurements using “ordinary” scattering cross-sections and do not require a completely opaque medium. Until such disagreements over the interpretation of the most basic high- $p_T$  measurement are resolved we cannot really claim to “understand” jet quenching.

This paper will use a selection of new results from Run 4 and Run 5 data-taking at RHIC to address many of the above questions/problems. The focus of the paper is on the evolution of jet quenching phenomena from intermediate to high  $p_T$ , the potential role of physics other than radiative energy loss, and our theoretical understanding of the measurements.

## 2. Single high- $p_T$ hadron production

An important feature of Au+Au jet quenching measurements is the approximate constancy of the observed single hadron suppression as a function of  $p_T$ . While early energy loss calculations [44] predicted a weakening of the single hadron suppression with increasing  $p_T$ , more recent energy loss analyses [45,6,40,43,39,42] can reproduce the approximate constancy of  $R_{AA}(p_T)$  via a combination of more exact calculation, shadowing, Cronin effect, “feedback” and absorption of energy from the medium [46,42], interplay of quark/gluon quenching, and the underlying shapes of the scattered parton spectra. Measurements of single hadron production at higher  $p_T$  where some of these effects are less important will be critical to understanding the apparent constancy of high- $p_T$  single hadron suppression. Clearly an important question is whether the “intrinsic” energy loss behavior – a decrease of the suppression with increasing  $p_T$  – will eventually be revealed. To address these points, Fig. 1 shows preliminary Run 4 PHENIX measurements of  $\pi^0$   $R_{AA}$  in 200 GeV Au+Au collisions in six centrality bins. These data show clearly the approximate constancy of the high- $p_T$   $\pi^0$  suppression in Au+Au collisions for *all* centralities. The suppression is approximately  $p_T$ -independent out to 20 GeV/c, though there is a suggestion of a gradual increase in the  $R_{AA}(p_T)$  with increasing  $p_T$  in the 0-10% and 0-5% centrality bins.

If we are to understand the  $p_T$  dependence of suppression in Au+Au collisions, we should

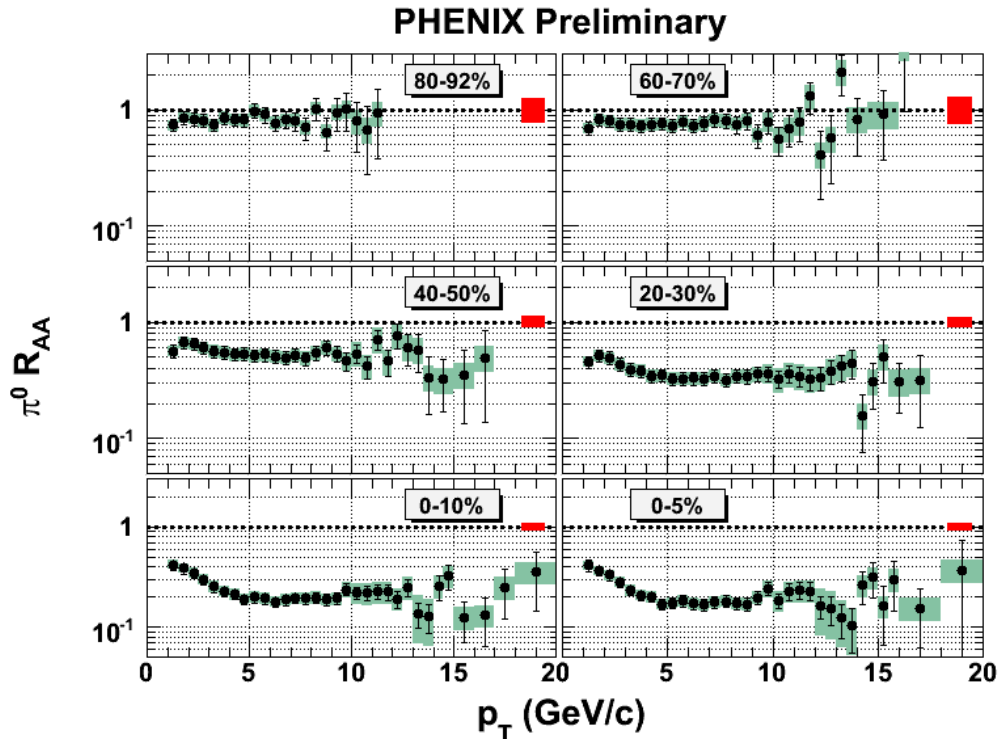


Figure 1. PHENIX Run 4  $\pi^0 R_{AA}(p_T)$  for 6 centrality bins in 200 GeV Au+Au collisions. The error bars (boxes) on the points show statistical (point-to-point systematic) errors. The Boxes on  $R_{AA} = 1$  line show separate multiplicative systematic errors.

first make sure we understand the  $p_T$  dependence of  $\pi^0$  production in d+Au collisions. To this end, final results from PHENIX measurements of  $\pi^0$  production in d+Au collisions are plotted in Fig. 2 for four different bins of collision centrality. These data show a centrality-dependent change in  $R_{dA}$  at high- $p_T$  that indicates a modest suppression in the yield of high  $p_T$   $\pi^0$ 's in central d+Au collisions relative to peripheral collisions. While the reduction of  $R_{dA}$  below 1 in central collisions is of modest significance when all errors are accounted for, the differences between the high- $p_T$   $R_{dA}$  values for peripheral and central collisions are much more significant. It is worth noting that STAR measurements are consistent with a decrease of  $R_{dA}$  below 1 for  $p_T > \sim 8$  GeV/c in central d+Au collisions [47]. Such a suppression could result from the EMC reduction in the Au nuclear parton distribution above  $x = 0.2$ , but only if the EMC effect is impact parameter dependent. The suppression might also be partially due to energy loss of quarks/gluons in the cold nucleus. Regardless of the explanation, we can reasonably expect that similar effects are also present in Au+Au collisions and that they affect the observed  $R_{AA}(p_T)$ . Without the contributions from this effect, we would then presumably see a (stronger) rise in  $\pi^0 R_{AA}$  with increasing  $p_T$ .

Figure 3 shows a comparison of the central Au+Au  $\pi^0 R_{AA}$  values from Fig. 1 to three different theoretical energy-loss calculations, PQM [39], GLV (Vitev), and a calculation by Turbide *et al.* using the AMY transport formalism [48,49]. The PQM calculation was obtained using three different values for the BDMPS transport coefficients [19],  $\hat{q} = 4, 10, 15$  GeV<sup>2</sup>/fm. The GLV calculations were performed for three different initial gluon  $dn/dy$  values, the largest shown only to demonstrate that the suppression

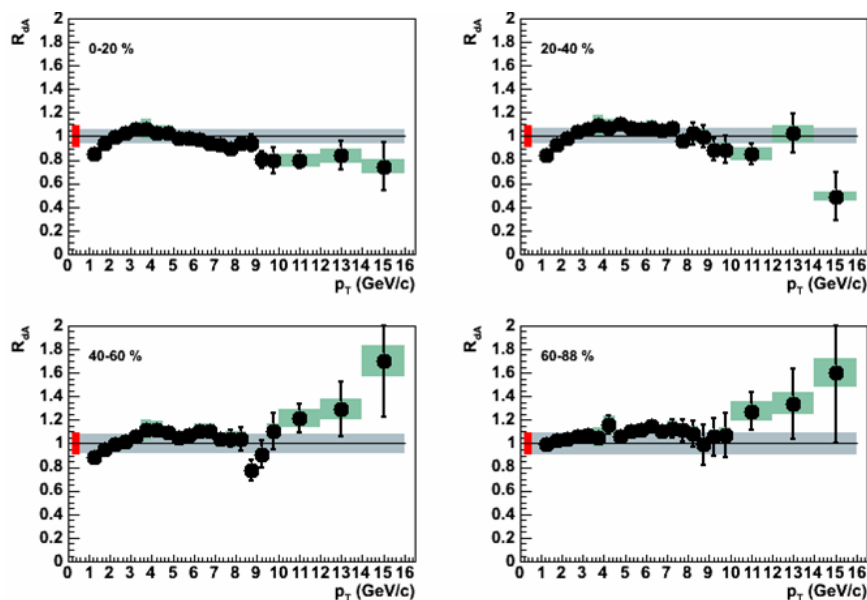


Figure 2. PHENIX final  $\pi^0$   $R_{dA}$  in 200 GeV d+Au collisions for 4 centrality bins. Error bars (boxes) on the data points show statistical (point-to-point systematic) errors. The band around  $R_{dA} = 1$  indicates a  $p_T$ -independent (multiplicative) systematic error.

in the GLV calculation(s) does not saturate with increased medium density. The AMY calculations use initial conditions,  $\tau_i \approx 0.15$  fm and  $T_i = 370$  MeV, corresponding to a produced particle  $dn/dy = 1260$ . The only other parameter in the AMY calculation is the strong coupling constant, and results are shown for two values of  $\alpha_s$ . As the figure demonstrates, all three calculations are capable of describing the  $p_T$  dependence of the single  $\pi^0$  suppression in central (0-10%) Au+Au collisions out to 20 GeV/c. There are subtle differences in the observed  $p_T$  dependence – particularly for the AMY calculation which appears to be turning down at high  $p_T$ . However, such differences in  $p_T$  dependence are difficult to assess since the three calculations use different nucleon PDF's, shadowing functions, Cronin effect parameterizations etc. The AMY calculations demonstrate the sensitivity of the energy loss to  $\alpha_s$ : a  $\approx 10\%$  change in  $\alpha_s$  produces a  $\approx 25\%$  change in the  $\pi^0$  suppression. Since  $\alpha_s$  is not known *a priori* to 10% accuracy, the strong coupling constant **must** contribute considerable systematic uncertainty in energy-loss calculations. The dependence of the AMY results on  $\alpha_s$  also provides insight on the sensitivity of  $\pi^0$   $R_{AA}$  to medium properties. If the medium is sufficiently opaque that the single hadron suppression becomes insensitive to medium properties, changing  $\alpha_s$  by 10% should not produce the observed reduction in  $\pi^0$   $R_{AA}$ . The calculations by Vitev also appear to show no saturation in  $\pi^0$   $R_{AA}$  with increasing medium density ( $dn_g/dy$ ). Both the AMY and GLV calculations use initial parton densities roughly consistent with final-state particle multiplicities. Thus, the loss of sensitivity of the single high- $p_T$  hadron  $R_{AA}$  to the properties of the medium and the extreme medium densities required to explain the data seem to be unique features of energy loss calculations based on BDMPS quenching weights.

Since, we don't know whether the vastly different interpretations of the Au+Au single hadron data are due to differences in the description of the energy loss process itself or due to differences in description of the geometry/time-evolution of the medium, Cu+Cu data

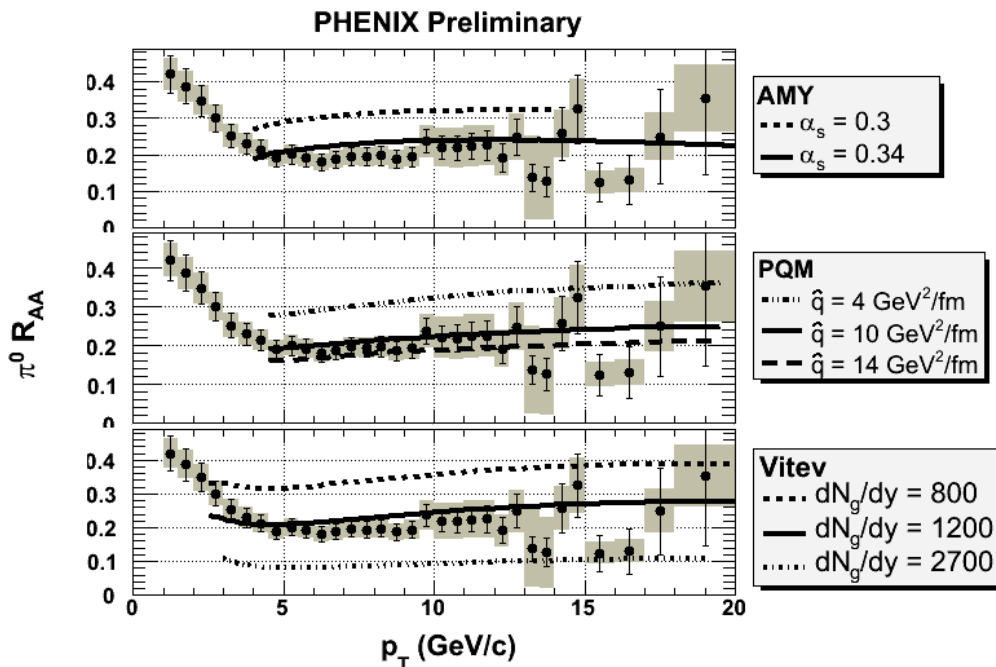


Figure 3. Comparison between PHENIX Run 4 measurements of  $\pi^0 R_{AA}$  in 200 GeV central (0-10%) Au+Au collisions and three energy loss calculations (see text for details).

could provide a valuable alternative test of the energy loss models. In Cu+Cu collisions the medium will be less opaque and we could hope that reasonable extrapolation of medium properties in the different calculations to Cu+Cu collisions would provide testable differences in predicted  $R_{AA}$ . However, preliminary measurements of  $\pi^0$  production by PHENIX [50] and charged hadron production by STAR [51] yield results that can be explained by both GLV (also see [43]) and PQM calculations. In fact, both GLV and PQM analyses suggest an  $N_{\text{part}}^{2/3}$  dependence of opacity on collision size/centrality, but for different reasons. This would suggest that calculations using BDMPs quenching weights uniformly require greater medium opacity than other calculations.

### 3. High- $p_T$ azimuthal anisotropy

As discussed above, measurements of hadron azimuthal anisotropy in the currently accessible  $p_T$  range cannot be explained purely by medium-induced radiative energy loss. However, contributions other than radiative energy loss may be largest at intermediate  $p_T$  so an extension of azimuthal anisotropy measurements to higher  $p_T$  may help constrain theoretical analyses and improve our understanding of the origin of the large anisotropies. To this end, Fig. 4 shows new Run 4 preliminary measurements from PHENIX of the  $p_T$  dependence of  $\pi^0 v_2$  in Au+Au collisions in the 20-30% centrality bin where the PHENIX reaction plane resolution is best (see [52] for more details). The data in Fig. 4 demonstrate a clear and statistically significant reduction in  $\pi^0 v_2$  with increasing  $p_T$  from a maximum at  $p_T \sim 3$  GeV/c. Also shown in Fig. 4 are results from two of the calculations discussed in Sec. 2, namely PQM and AMY. The comparison between the data and calculations in Fig. 4 demonstrates the inability of “standard” energy loss models to reproduce the large  $v_2$  observed at moderate  $p_T$ ,  $p_T < \sim 6$  GeV/c. However, the figure also shows that

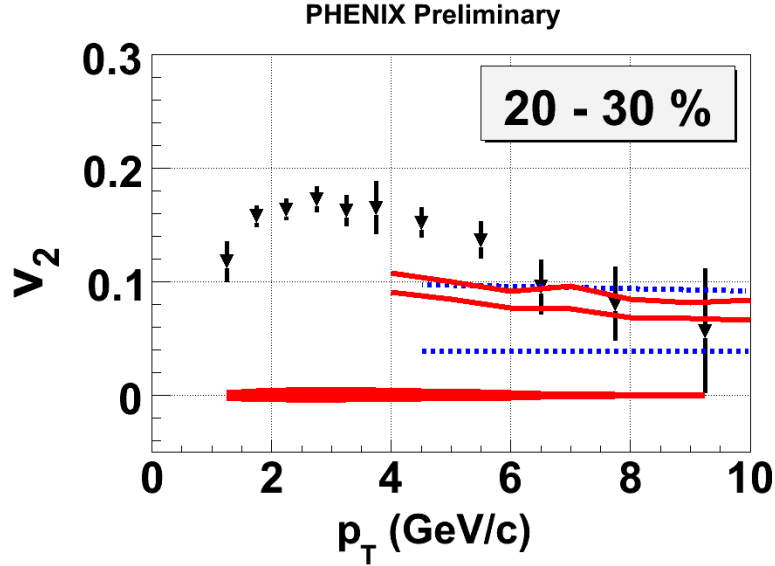


Figure 4. PHENIX  $\pi^0$   $v_2(p_T)$  in 200 GeV Au+Au collisions (20-30% centrality). Curves show energy loss calculations: solid - AMY (20-40% centrality), dashed - PQM.

at larger  $p_T$ , the measured  $\pi^0$   $v_2$  decreases to a value consistent with radiative energy loss calculations. Thus, the measurements suggest that for  $p_T > \sim 6$  GeV/c, the azimuthal anisotropy can be understood completely on the basis of radiative energy loss.

To understand the origin of the enhanced  $v_2$  at intermediate  $p_T$ , we should investigate more closely the dependence of the  $\pi^0$  suppression on  $\Delta\phi$ , the angle of the  $\pi^0$  wrt the reaction plane. Since the mechanism responsible for the larger  $v_2$  may also influence the  $\Delta\phi$ -integrated yield, separate studies of  $R_{AA}$  and  $v_2$  may miss important experimental clues to the origin of the azimuthal anisotropy at intermediate  $p_T$ . Figure 5 shows PHENIX measurements of  $\pi^0$   $R_{AA}(p_T)$  in six  $\Delta\phi$  bins covering  $0 < \Delta\phi < 90^\circ$ . The measured  $R_{AA}(p_T)$  is constant for  $\pi^0$  production nearly perpendicular to the reaction plane ( $75^\circ < \Delta\phi < 90^\circ$ ), while  $R_{AA}(p_T)$  increases rapidly with decreasing  $p_T$  for  $\pi^0$  production in the reaction plane ( $0 < \Delta\phi < 15^\circ$ ). As suggested above, these results indicate a strong correlation between the  $\Delta\phi$ -integrated  $R_{AA}$  and  $v_2$ , since the increase in yield ( $R_{AA}$ ) in the in-plane  $\Delta\phi$  bin(s) is not offset by a decrease in yield in the out-of-plane bin(s). Given the energy loss calculations shown in Fig's 3 & 4, it is reasonable to infer that the flat  $R_{AA}(p_T)$  in the out-of-plane bin reflects the intrinsic  $p_T$  dependence of the energy loss process. This inference is also supported by the results in Fig. 5 in the central (0-10%) bin for which  $R_{AA}(p_T)$  is approximately constant above 4 GeV/c for all  $\Delta\phi$  bins. Then, we might conclude that the mechanism responsible for the large  $v_2$  at intermediate  $p_T$  must generate “extra” partons/hadrons in the direction of the reaction plane. The process suggested by Molnar [30] in which multiple scattering in the medium boosts soft partons to high- $p_T$  provides an example of just such a mechanism. In contrast, the mechanism suggested by Armesto *et al.* in which the energy loss (suppression) is larger for partons ( $\pi^0$ ) moving across the flow field (out of plane) and smaller for partons ( $\pi^0$ ) moving parallel to the flow field (in plane) would appear to be inconsistent with the data. However, strong conclusions should await more detailed and systematic model comparisons with the data, particularly because of the potential subtlety of the interaction between transverse

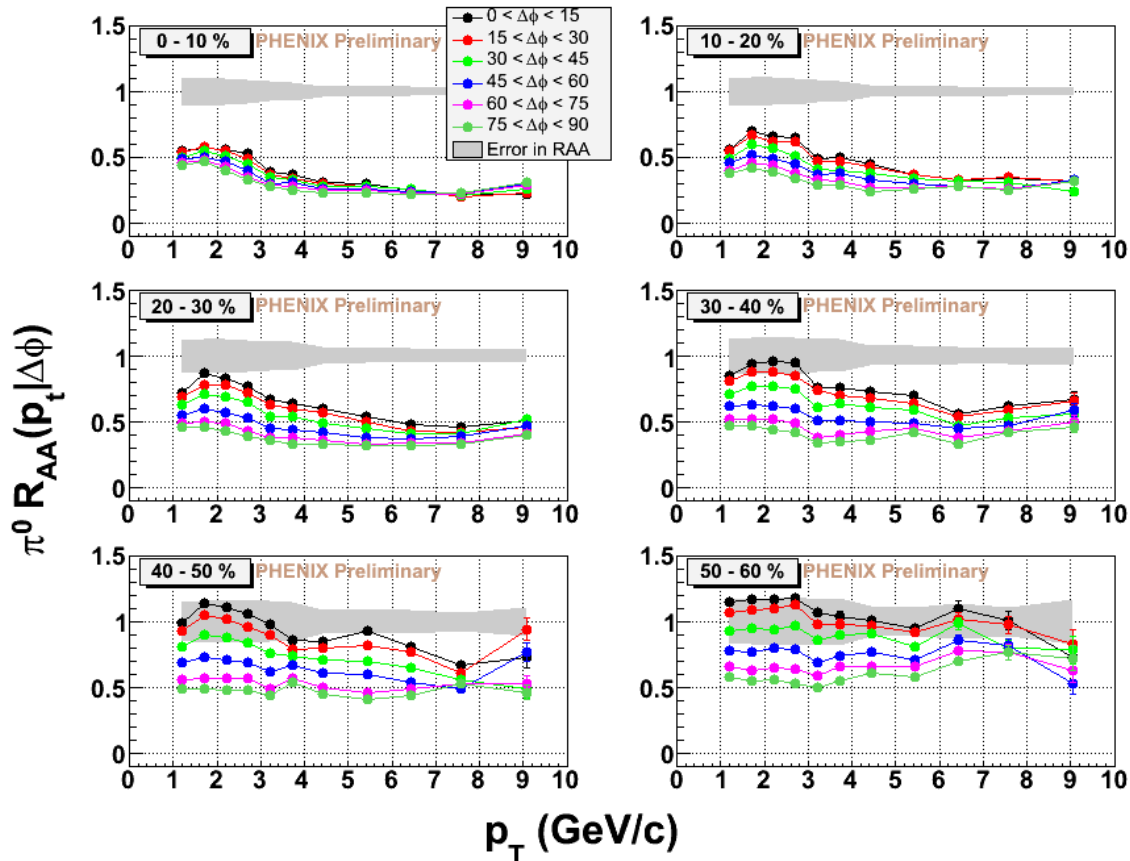


Figure 5. PHENIX Run 4  $\pi^0 R_{AA}(p_T|\Delta\phi)$  in 6 centrality bins. The shaded region around  $R_{AA} = 1$  reflects the systematic errors due to the reaction plane resolution correction.

flow and energy loss [41]. Nonetheless, measurements like those in Fig. 5 should provide stringent tests of calculations of azimuthal anisotropy and flow-dependent quenching.

#### 4. Jet Correlations at intermediate $p_T$

Di-hadron correlations provide a completely different tool for studying jet quenching in heavy ion collisions. For the purposes of this paper, only results at intermediate  $p_T$  will be considered; discussions of other aspects of jet correlation analyses can be found elsewhere in these proceedings. The most prominent feature of di-hadron correlations at intermediate  $p_T$  is the strong distortion of the di-jet signal first reported by PHENIX [17]. This result is critically important given its possible interpretation in terms of a “Mach cone”, Cherenkov radiation, etc. On the experimental side, the measurement is difficult due to the required subtraction of substantial flow-modulated background. Errors in the description of the background can distort the shape of the extract di-jet signal so verification of the di-jet modification is essential given the importance of the result.

Figure 6 shows PHENIX Run 4 measurements of di-hadron  $\Delta\phi$  correlations in central (0-10%) Au+Au collisions for four different bins in trigger and associated hadron  $p_T$  (see[53] for more details). The modification of the di-jet signal is so strong that it can be seen in the lowest  $p_T$  bin prior to background subtraction. After background subtraction we find a “saddle” shape with peaks at  $\Delta\phi = \pi \pm \approx 1$  consistent with the first PHENIX

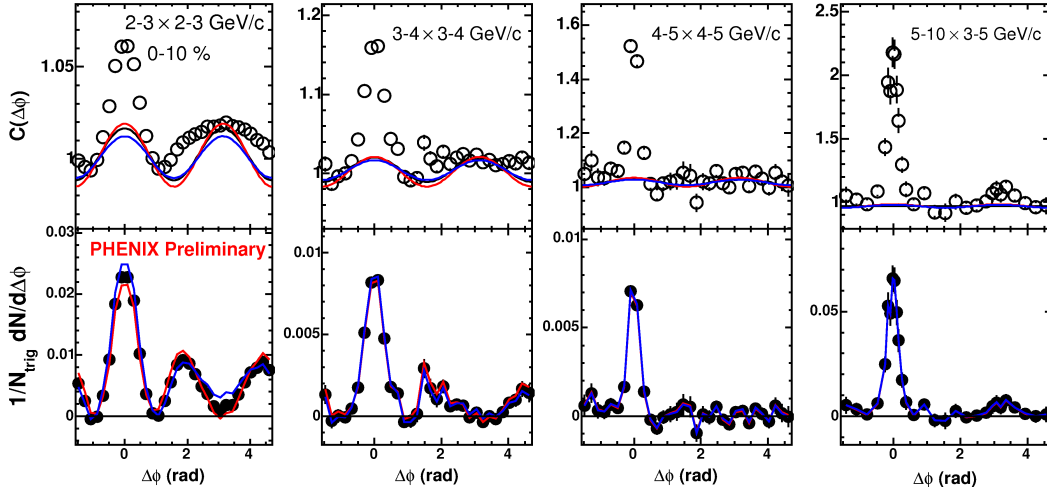


Figure 6. PHENIX Run 4 di-hadron correlation functions (top) and yields per trigger (bottom) in various trigger, associated  $p_T$  bins in central (0-10%) Au+Au collisions. Solid curves, top: estimated background with  $1\text{-}\sigma$  syst. errors.

results [17]. With increasing  $p_T$ , the contributions from the “saddle” decrease and in the highest  $p_T$  bin in Fig. 6 a hint of the true di-jet signal can be observed. Figure 7 shows preliminary STAR measurements [54] in  $p_T$  bins that match the original PHENIX publication. While the reduction in yield in the STAR di-hadron  $\Delta\phi$  distributions at  $\Delta\phi = \pi$  is weaker than in the PHENIX results, the qualitative features are the same – a strong production of associated hadrons peaked at  $\Delta\phi \approx 2$  and a reduction near  $\Delta\phi = \pi$ . Conclusions regarding possible differences between the STAR and PHENIX results must await more detailed comparisons and cross-checks on background subtraction techniques.

An alternative method for checking PHENIX background subtracted di-hadron correlation measurements was developed by J. Jia [53] in which the di-hadron correlation function and associated yields are measured as a function of  $\Delta\phi^{\text{trig}}$ , the angle of the trigger hadron *wrt* reaction plane. The results of this analysis for six reaction plane angle bins in the range  $0 < \Delta\phi^{\text{trig}} < 90^\circ$  are shown in Fig. 8. The points with the largest modulation correspond to  $0 < \Delta\phi^{\text{trig}} < 15^\circ$  while the points with the smallest modulation correspond to  $75^\circ < \Delta\phi^{\text{trig}} < 90^\circ$ . The other  $\Delta\phi^{\text{trig}}$  bins smoothly interpolate between these extremes. This reaction plane dependent analysis is useful because the shape of the elliptic flow modulation changes completely as a function of  $\Delta\phi^{\text{trig}}$  [55]. In fact, it is difficult to observe anything other than the flow modulation in the correlation functions in Fig. 8. However, once the correct  $\Delta\phi^{\text{trig}}$ -dependent flow-modulated background is subtracted, the associated hadron yields shown in the right panel of Fig. 8 are all consistent and show the “saddle” structure seen in the original PHENIX paper. The slight differences between the results for the different reaction plane bins in Fig. 8 are known to partially result from an unsubtracted  $\cos(4\Delta\phi)$  term in the background but may also reflect contributions from reaction plane dependence of the di-jet distortion. Based on the results in Fig. 8 we can conclude that such a dependence is small. The results in Fig. 8 provide strong validation that the PHENIX di-hadron measurement at intermediate  $p_T$  is under good systematic control. Even small errors in  $v_2$  and/or average background level would produce substantial differences in the shape of the  $\Delta\phi$  distributions for different  $\Delta\phi^{\text{trig}}$ .

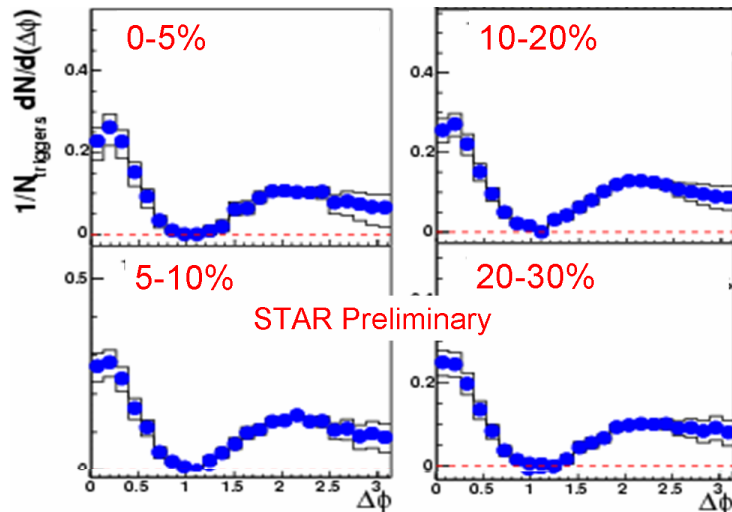


Figure 7. STAR Run 4 di-hadron yields vs.  $\Delta\phi$  in 200 GeV Au+Au collisions for  $2.5 < p_T^{\text{trig}} < 4$  GeV/c and  $1 < p_T^{\text{assoc}} < 2.5$  GeV/c. The solid curves indicate systematic uncertainties in the background subtraction.

With the qualitative agreement between (preliminary) STAR and PHENIX results established and the above-described systematic checks on the PHENIX measurements performed, we can now focus on understanding the origin of the di-jet modification. Possible interpretations and further experimental analyses of the effect can be found elsewhere in these proceedings. The strong di-jet distortion is clearly one of the most compelling “high- $p_T$ ” problems at RHIC and an understanding of the effect will provide valuable new insight on the physics of a colored charge propagating in a dense colored medium. More details on these analyses can be found elsewhere in these proceedings [56–59].

## 5. Photon-hadron correlations

Photon-jet processes have been the “holy grail” of the RHIC high- $p_T$  community for nearly a decade because of the potential sensitivity they provide to medium-induced energy loss [60]. Such measurements have previously been unfeasible due to the low rate of

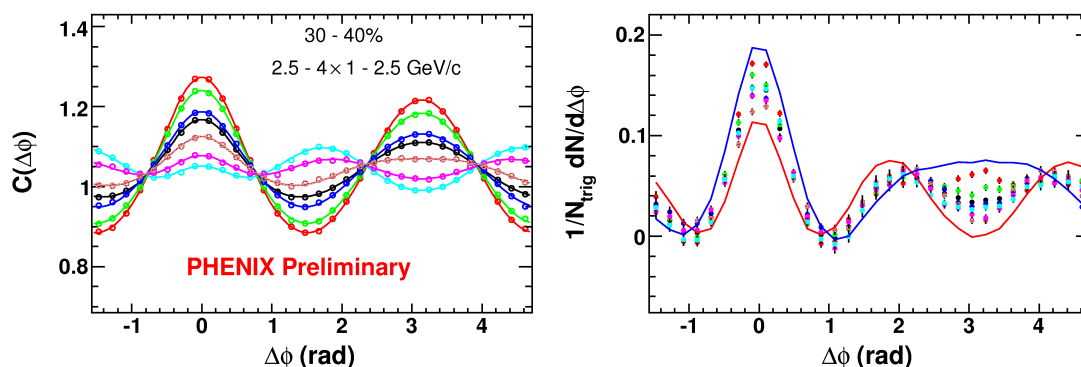


Figure 8. PHENIX Run 4 Preliminary di-hadron correlation functions (left) and associated hadron yields per trigger (right) in 30-40% centrality 200 GeV Au+Au collisions for six bins in  $\Delta\phi^{\text{trig}}$  and  $\Delta\phi^{\text{trig}}$ -integrated (see text for more details).

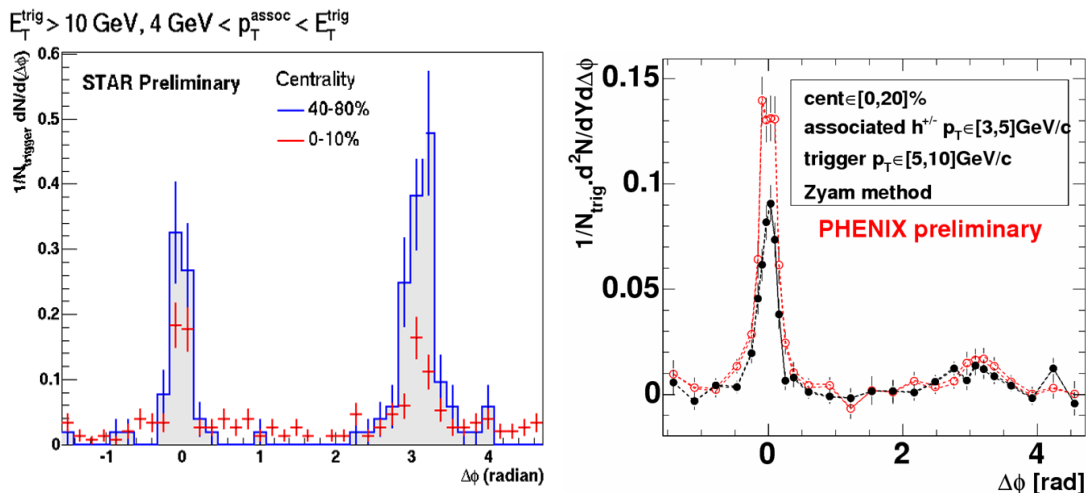


Figure 9. Inclusive  $\gamma$ -hadron per-trigger associated hadron yields vs  $\Delta\phi$  in shown  $p_T$  bins. Left: STAR, right: PHENIX  $\circ$  -  $\gamma$  triggers,  $\bullet$  -  $\pi^0$  triggers,

photon-jet processes, but with the increased Au+Au statistics available from Run 4, both STAR and PHENIX have initiated photon-hadron correlation studies. Inclusive photon-hadron correlation measurements shown in Fig. 9 for 200 GeV Au+Au collision from both PHENIX [61] and STAR [62] show clear evidence of prompt photon contributions. The STAR data show a reduced yield of hadrons produced at small angles *wrt* photons with  $p_T > 10$  GeV/c in central collisions relative to peripheral collisions. The PHENIX data show a reduced yield of hadrons produced at small angles *wrt* trigger photons relative to trigger  $\pi^0$ 's. In both cases, the reduced yield is consistent with a relatively large prompt photon contribution [5] in central collisions. For now, measurements like those shown in Fig. 9 are only exploratory. Nonetheless, they represent the first step down the path to true photon-jet measurements at RHIC.

## 6. Summary

New results presented at the Quark Matter 2005 conference have provided substantial advances in our experimental knowledge base on high- $p_T$  hadron production and jet quenching. We now know that the factor of 4 – 5 single-hadron suppression in central Au+Au collisions persists unchanged out to  $p_T = 20$  GeV/c though the Run 4  $\pi^0$  measurements from PHENIX suggest a slow growth of  $R_{AA}$  with  $p_T$ . New d+Au  $\pi^0$  results at high  $p_T$  may provide the first direct observation of nuclear PDF modifications and/or parton energy loss in the cold nucleus. New Cu+Cu measurements show significant single hadron suppression with a dependence on  $N_{part}$  that is similar to, if not completely consistent with Au+Au results. New measurements of  $\pi^0$  azimuthal anisotropy show that  $v_2$  decreases from a maximum near  $p_T = 3$  GeV/c to a value  $\lesssim 0.1$  near  $p_T = 10$  GeV/c. The high quality data available from Run 4 now allow direct studies of single hadron production/suppression on the angle of the hadron *wrt* reaction plane. The recent observation of strong modification of the di-jet signal has opened an entirely new chapter in the study of parton propagation in a strongly interacting medium. New results from Run 4 presented here provide strong confirmation that the effect is not an experimental artifact. When the effect is understood we will surely learn more about medium properties and the physics

of a colored parton propagating in a dense, colored medium.

Energy loss calculations successfully describe both the  $p_T$  and  $N_{\text{part}}$  dependence of single-hadron suppression in both Au+Au and Cu+Cu collisions. The  $\pi^0$   $v_2$  at high  $p_T$  is consistent with radiative energy loss calculations suggesting that azimuthal anisotropy measurements may provide real tomographic information about the medium. However, our enthusiasm at the success of energy loss calculations must be tempered by recognition of the vastly different conclusions regarding the opacity of the medium drawn from different energy loss calculations. Clearly we need to find better ways to experimentally test the different ingredients of these calculations. While di-jet measurements [63] provide new information, even two observables,  $R_{AA}$  and  $I_{AA}$ , will not suffice to resolve disagreements in the description of the basic energy loss process *and* constrain collisional energy loss *and* elucidate transverse and longitudinal flow effects *and* constrain “soft” contributions at high  $p_T$ , *and* test the sensitivity of jet quenching to the geometry of the medium, *and* constrain final-state hadronic absorption contributions *and* ... It is essential that measurements of azimuthal anisotropy, di-jet quenching, jet  $(\eta, \phi)$  profile, etc. be extended to  $p_T > 10$  GeV/c where radiative energy loss may be dominant. With the addition of heavy quark studies, future photon-jet results, di-jet modification and new, clever measurements not yet anticipated we may still hope to unravel the complicated mix of physics contributing to jet quenching and improve our sensitivity to medium properties.

## 7. Acknowledgements

This work was supported by the US Department of Energy under grant DE-FG02-86ER40281. I would like to acknowledge substantial contributions by S. Mioduszewski and J. Jia to the ideas and insights presented in this paper.

## REFERENCES

1. PHENIX, K. Adcox *et al.*, Nucl. Phys. **A757**, 184 (2005), nucl-ex/0410003.
2. STAR, J. Adams *et al.*, Nucl. Phys. **A757**, 102 (2005), nucl-ex/0501009.
3. BRAHMS, I. Arsene *et al.*, Nucl. Phys. **A757**, 1 (2005), nucl-ex/0410020.
4. PHOBOS, B. B. Back *et al.*, Nucl. Phys. **A757**, 28 (2005), nucl-ex/0410022.
5. PHENIX, S. S. Adler *et al.*, Phys. Rev. Lett. **94**, 232301 (2005), nucl-ex/0503003.
6. I. Vitev and M. Gyulassy, Phys. Rev. Lett. **89**, 252301 (2002), hep-ph/0209161.
7. M. Gyulassy and L. McLerran, Nucl. Phys. **A750**, 30 (2005), nucl-th/0405013.
8. X.-N. Wang, Nucl. Phys. **A750**, 98 (2005), nucl-th/0405017.
9. V. M. Bannur, Eur. Phys. J. **C11**, 169 (1999), hep-ph/9811397.
10. E. V. Shuryak and I. Zahed, Phys. Rev. **C70**, 021901 (2004), hep-ph/0307267.
11. E. Shuryak, J. Phys. **G30**, S1221 (2004).
12. I. Zahed, J. Phys. **G30**, S1267 (2004).
13. M. Gyulassy, (2004), nucl-th/0403032.
14. B. Muller, (2004), nucl-th/0404015.
15. E. V. Shuryak, Nucl. Phys. **A750**, 64 (2005), hep-ph/0405066.
16. STAR, J. Adams *et al.*, (2004), nucl-ex/0411003.
17. PHENIX, S. S. Adler *et al.*, (2005), nucl-ex/0507004.
18. X.-N. Wang, M. Gyulassy, and M. Plumer, Phys. Rev. **D51**, 3436 (1995).
19. R. Baier *et al.*, Nucl. Phys. **B483**, 291 (1997), hep-ph/9607355.

20. B. G. Zakharov, JETP Lett. **65**, 615 (1997), hep-ph/9704255.
21. M. Gyulassy, P. Levai, and I. Vitev, Phys. Rev. Lett. **85**, 5535 (2000).
22. B. G. Zakharov, JETP Lett. **80**, 617 (2004), hep-ph/0410321.
23. M. H. Thoma, J. Phys. **G26**, 1507 (2000), hep-ph/0003016.
24. M. G. Mustafa and M. H. Thoma, Acta Phys. Hung. **A22**, 93 (2005), hep-ph/0311168.
25. M. G. Mustafa, Phys. Rev. **C72**, 014905 (2005), hep-ph/0412402.
26. G. D. Moore and D. Teaney, Phys. Rev. **C71**, 064904 (2005), hep-ph/0412346.
27. N. Borghini and U. A. Wiedemann, (2005), hep-ph/0506218.
28. E. V. Shuryak and I. Zahed, Phys. Rev. **D67**, 054025 (2003), hep-ph/0207163.
29. T. S. Biro and G. Purcsel, (2005), hep-ph/0503204.
30. D. Molnar, (2005), nucl-th/0503051.
31. X.-N. Wang, Phys. Rev. **C63**, 054902 (2001), nucl-th/0009019.
32. E. V. Shuryak, Phys. Rev. **C66**, 027902 (2002), nucl-th/0112042.
33. B. Muller, Phys. Rev. **C67**, 061901 (2003), nucl-th/0208038.
34. A. Drees, H. Feng, and J. Jia, Phys. Rev. **C71**, 034909 (2005), nucl-th/0310044.
35. R. J. Fries *et al.*, Phys. Rev. **C68**, 044902 (2003), nucl-th/0306027.
36. V. Greco, C. M. Ko, and P. Levai, Phys. Rev. **C68**, 034904 (2003), nucl-th/0305024.
37. N. Armesto, C. A. Salgado, and U. A. Wiedemann, Phys. Rev. Lett. **93**, 242301 (2004), hep-ph/0405301.
38. W. A. Horowitz, nucl-th/0511052, QM2005 poster proceedings.
39. A. Dainese, C. Loizides, and G. Paic, Eur. Phys. J. **C38**, 461 (2005), hep-ph/0406201.
40. K. J. Eskola *et al.*, Nucl. Phys. **A747**, 511 (2005), hep-ph/0406319.
41. T. Renk and J. Ruppert, Phys. Rev. **C72**, 044901 (2005), hep-ph/0507075.
42. S. Turbide *et al.*, Phys. Rev. **C72**, 014906 (2005), hep-ph/0502248.
43. X.-N. Wang, Phys. Lett. **B595**, 165 (2004), nucl-th/0305010.
44. S. A. Bass *et al.*, Nucl. Phys. **A661**, 205 (1999), nucl-th/9907090.
45. P. Levai *et al.*, Nucl. Phys. **A698**, 631 (2002), nucl-th/0104035.
46. E. Wang and X.-N. Wang, Phys. Rev. Lett. **87**, 142301 (2001), nucl-th/0106043.
47. STAR, J. Adams *et al.*, Phys. Rev. Lett. **91**, 072304 (2003), nucl-ex/0306024.
48. P. Arnold, G. D. Moore, and L. G. Yaffe, JHEP **11**, 057 (2001), hep-ph/0109064.
49. P. Arnold, G. D. Moore, and L. G. Yaffe, JHEP **06**, 030 (2002), hep-ph/0204343.
50. PHENIX, M. Shimomura, nucl-ex/0510023, these proceedings.
51. STAR, J. C. Dunlop, nucl-ex/0510073, these proceedings.
52. PHENIX, D. Winter, nucl-ex/0511039, these proceedings.
53. PHENIX, J. Jia, nucl-ex/0510060, QM2005 poster proceedings.
54. STAR, M. Horner, QM2005 poster proceedings.
55. J. Bielcikova *et al.*, Phys. Rev. **C69**, 021901 (2004), nucl-ex/0311007.
56. J. Ruppert, hep-ph/0509133, these proceedings.
57. PHENIX, N. Grau, nucl-ex/0511046, these proceedings.
58. STAR, F. Wang, nucl-ex/0510068, these proceedings.
59. PHENIX, H. Buesching, nucl-ex/0511044, these proceedings.
60. X.-N. Wang, Z. Huang, and I. Sarcevic, Phys. Rev. Lett. **77**, 231 (1996).
61. PHENIX, J. Jin, QM2005 poster proceedings.
62. STAR, T. Dietel, nucl-ex/0510046, these proceedings.
63. P. M. Jacobs and M. van Leeuwen, nucl-ex/0511013, these proceedings.